

A Closed-Form Full-State Feedback Controller for Stabilization of 3D Magnetohydrodynamic Channel Flow

Rafael Vazquez¹

Departamento de Ingeniería Aeroespacial,
Universidad de Sevilla,
Camino de los Descubrimientos,
41092 Sevilla, Spain
e-mail: rvazquez1@us.es

Eugenio Schuster

Department of Mechanical Engineering and
Mechanics,
Lehigh University,
Bethlehem, PA 18015-3085
e-mail: schuster@lehigh.edu

Miroslav Krstic

Department of Mechanical and Aerospace
Engineering,
University of California, San Diego,
La Jolla, CA 92093-0411
e-mail: krstic@ucsd.edu

We present a boundary feedback law that stabilizes the velocity, pressure, and electromagnetic fields in a magnetohydrodynamic (MHD) channel flow. The MHD channel flow, also known as Hartmann flow, is a benchmark for applications such as cooling, hypersonic flight, and propulsion. It involves an electrically conducting fluid moving between parallel plates in the presence of an externally imposed transverse magnetic field. The system is described by the inductionless MHD equations, a combination of the Navier–Stokes equations and a Poisson equation for the electric potential under the MHD approximation in a low magnetic Reynolds number regime. This model is unstable for large Reynolds numbers and is stabilized by actuation of velocity and the electric potential at only one of the walls. The backstepping method for stabilization of parabolic partial differential equations (PDEs) is applied to the velocity field system written in appropriate coordinates. Control gains are computed by solving a set of linear hyperbolic PDEs. Stabilization of nondiscretized 3D MHD channel flow has so far been an open problem. [DOI: 10.1115/1.3089561]

1 Introduction

In this paper, we derive an explicit boundary controller that stabilizes an incompressible magnetohydrodynamic (MHD) flow in an infinite rectangular 3D channel. Known as the Hartmann flow [1], this model is considered a benchmark for applications such as liquid-metal cooling of nuclear reactors and supercomputers, plasma confinement, electromagnetic casting, hypersonic flight, and propulsion.

In the Hartmann flow, an electrically conducting fluid (such as a liquid metal, a plasma, or salt water) moves between parallel plates and is affected by an imposed transverse magnetic field. The movement of a conducting fluid produces an electric field and subsequently an electric current. The interaction between this current and the external magnetic field induces a body force, called the Lorentz force, which acts on the fluid itself. Hence the velocity and electromagnetic fields are highly coupled. These fields are mathematically described by the MHD equations [2], which are the Navier–Stokes equation coupled with the Maxwell equations.

In the nonconducting case, the geometry we consider (channel flow) is known to be unstable for high Reynolds numbers and has been thoroughly studied and is frequently cited as a paradigm for transition to turbulence [3]. There are many works in flow control that consider the problem of channel flow stabilization, for instance, using optimal control [4], backstepping [5,6], spectral decomposition/pole placement [7], Lyapunov design/passivity [8,9], or nonlinear model reduction/in-domain actuation [10].

The stability of the Hartmann flow has also been extensively studied, both from the numerical and the analytical point of view [11–14]. However, specific results on stabilization of magnetohydrodynamic flows are more scarce. Prior works focus mainly on

electromagnetohydrodynamic (EMHD) flow control in weak electrically conducting fluids such as salt water. Traditionally two types of actuator designs have been used: one type generates a Lorentz field parallel to the wall in the streamwise direction [15], while the other generates a Lorentz field normal to the wall in the spanwise direction [16,17]. EMHD flow control has been dominated by strategies that either permanently activate the actuators or pulse them at arbitrary frequencies. However, it has been shown that feedback control schemes can improve the efficiency, by reducing control power, for both streamwise [18] and spanwise [19,20] approaches. Other recent developments use model-based techniques, for instance, using nonlinear model reduction [21,22] or optimal control [23]. There are some experimental results available as well, showing the feasibility of MHD flow control; actuators consist of magnets and electrodes [16,17,24], for instance, electromagnetic tiles [25]. Mathematical studies of controllability of magnetohydrodynamic flows have been done, though they do not provide explicit controllers [26,27].

Applications include drag reduction [16,20], boundary layer control [25,28], mixing enhancement for cooling systems [29,30], turbulence control [31], or estimation of velocity, pressure, and electromagnetic fields [32].

This paper uses the backstepping method and extends our previous work for stabilization of the velocity field in a (nonconducting) 3D channel flow [6]. It also extends to three dimensions our past efforts for the 2D Hartmann flow [33]. None of these extensions are trivial since the growing number of states (three components of the velocity field, the electric field, and the pressure field, all infinite dimensional, evolving in an infinite 3D region) make the problem very challenging.

Our controller is designed for the continuum MHD model. Since the system is spatially invariant [34], control synthesis is done in the wave number space after application of a Fourier transform. Large wave numbers are found to be stable and left uncontrolled, whereas for small wave numbers control is used. For these wave numbers, control is used to put the system in a strict-feedback form; this is necessary for application of the back-

¹Corresponding author.

Contributed by the Dynamic Systems, Measurement, and Control Division of ASME for publication in the JOURNAL OF DYNAMIC SYSTEMS, MEASUREMENT, AND CONTROL. Manuscript received June 5, 2008; final manuscript received December 15, 2008; published online April 27, 2009. Assoc. Editor: Santosh Devasia.

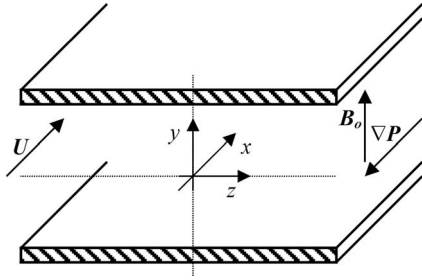


Fig. 1 Hartmann flow

stepping method for stabilization of parabolic partial differential equations (PDEs) [35]. Writing the velocity field in some appropriate coordinates, the resulting system is very similar to the Orr–Sommerfeld–Squire system of PDEs for nonconducting fluids and presents the same difficulties (non-normality leading to a large transient growth mechanism [36,37]). Thus, applying the same ideas as in Ref. [6], we use backstepping not only to guarantee stability but also to decouple the system in order to prevent transients. The control gains are computed by solving a set of linear hyperbolic PDEs—a much simpler task than, for instance, solving nonlinear operator Riccati equations. Actuation of velocity and electric potential is done at only one of the channel walls. Full-state knowledge is assumed, but the controller can be combined with an observer for MHD channel flow [32], which is a dual to the controller design in the present paper, to obtain an output feedback controller.

This paper is organized as follows. Section 2 introduces the governing equations. The equilibrium profile is presented in Sec. 3, and the linearized plant in wave number space is introduced in Sec. 4. Section 5 presents the design of the control laws to guarantee stability of the closed-loop system and states the main result. We end the paper with concluding remarks in Sec. 6.

2 Model

Consider an incompressible conducting fluid enclosed between two plates, separated by a distance L , under the influence of a pressure gradient ∇P and a magnetic field B_0 normal to the walls, as shown in Fig. 1. Under the assumption of a very small magnetic Reynolds number

$$\text{Re}_M = \nu \rho \sigma U_0 L \ll 1 \quad (1)$$

where ν is the viscosity of the fluid, ρ is the density of the fluid, σ is the conductivity of the fluid, and U_0 is the reference velocity (maximum velocity of the equilibrium profile), the dynamics of the magnetic field can be neglected, and the dimensionless velocity and electric potential field is governed by the inductionless MHD equations [38].

We set nondimensional coordinates (x, y, z) , where x is the streamwise direction (parallel to the pressure gradient), y is the wall-normal direction (parallel to the magnetic field), and z is the spanwise direction so that $(x, y, z) \in (-\infty, \infty) \times [0, 1] \times (-\infty, \infty)$.² The governing equations are

$$U_t = \frac{\Delta U}{\text{Re}} - UU_x - VU_y - WU_z - P_x + N\phi_z - NU \quad (2)$$

$$V_t = \frac{\Delta V}{\text{Re}} - UV_x - VV_y - WV_z - P_y \quad (3)$$

$$W_t = \frac{\Delta W}{\text{Re}} - UW_x - VW_y - WW_z - P_z - N\phi_x - NW \quad (4)$$

²Our approach can be extended to finite periodic channels with only some changes; see, e.g., Ref. [39] for techniques involved.

$$\Delta \phi = U_z - W_x \quad (5)$$

where U , V , and W denote, respectively, the streamwise, wall-normal, and spanwise velocities, P is the pressure, ϕ is the electric potential, $\text{Re} = U_0 L / \nu$ is the Reynolds number, and $N = \sigma L B_0^2 / \rho U_0$ is the Stuart number. Since the fluid is incompressible, the continuity equation is verified,

$$U_x + V_y + W_z = 0 \quad (6)$$

The boundary conditions for the velocity field are

$$U(t, x, 0, z) = 0, \quad U(t, x, 1, z) = U_c(t, x, z) \quad (7)$$

$$V(t, x, 0, z) = 0, \quad V(t, x, 1, z) = V_c(t, x, z) \quad (8)$$

$$W(t, x, 0, z) = 0, \quad W(t, x, 1, z) = W_c(t, x, z) \quad (9)$$

where $U_c(t, x, z)$, $V_c(t, x, z)$, and $W_c(t, x, z)$ denote, respectively, the actuators for streamwise, wall-normal, and spanwise velocities in the upper wall. We denote the initial conditions for the velocity field as $U_0(x, y, z) = U(0, x, y, z)$, $V_0(x, y, z) = V(0, x, y, z)$, and $W_0(x, y, z) = W(0, x, y, z)$.

Assuming perfectly conducting walls, the electric potential must verify

$$\phi(t, x, 0, z) = 0, \quad \phi(t, x, 1, z) = \Phi_c(t, x, z) \quad (10)$$

where $\Phi_c(t, x, z)$ is the imposed potential (electromagnetic actuation) in the upper wall. The nondimensional electric current, $j(t, x, y, z)$, a vector field that is computed from the electric potential and velocity fields, is as follows:

$$j^x(t, x, y, z) = -\phi_x - W \quad (11)$$

$$j^y(t, x, y, z) = -\phi_y \quad (12)$$

$$j^z(t, x, y, z) = -\phi_z + U \quad (13)$$

where j^x , j^y , and j^z denote the components of j .

We assume that all actuators can be independently actuated for every $(x, z) \in \mathbb{R}^2$. Note that no actuation is done inside the channel or at the bottom wall.

3 Equilibrium Profile

The equilibrium profile for system (2)–(5) with no control can be calculated following the same steps that yield the Poiseuille solution for Navier–Stokes channel flow. Thus, we assume a steady solution with only one nonzero nondimensional velocity component, $U^e(y)$, that depends only on the y coordinate. Substituting $U^e(y)$ into Eq. (2), one finds that it verifies the following equation:

$$0 = \frac{U_{yy}^e(y)}{\text{Re}} - P_x^e - NU^e(y) \quad (14)$$

whose nondimensional solution is, setting P^e such that the maximum velocity (centerline velocity) is unity,

$$U^e(y) = \frac{\sinh(H(1-y)) - \sinh H + \sinh(Hy)}{2 \sinh H/2 - \sinh H} \quad (15)$$

$$V^e = W^e = \phi^e = 0 \quad (16)$$

$$P^e = \frac{N \sinh H}{2 \sinh H/2 - \sinh H} x \quad (17)$$

$$j^{xe} = j^{ye} = 0, \quad j^{ze} = U^e(y) \quad (18)$$

where $H = \sqrt{\text{Re} N} = B_0 L \sqrt{\sigma / \rho \nu}$ is the Hartmann number. In Fig. 2 (left) we show $U^e(y)$ for different values of H . Since the equilibrium profile is nondimensional the centerline velocity is always 1. For $H=0$ the classic parabolic Poiseuille profile is recovered. In Fig. 2 (right) we show $U_y^e(y)$, proportional to shear stress, whose

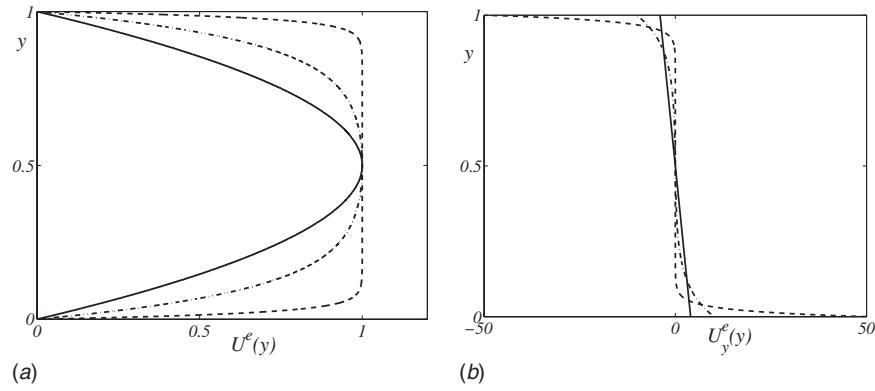


Fig. 2 Streamwise equilibrium velocity $U^e(y)$ (left) and $U_y^e(y)$ (right) for different values of H . Solid, $H=0$; dash-dotted, $H=10$; and dashed, $H=50$.

maximum is reached at the boundaries and grows with H .

4 The Plant in Wave Number Space

Define the fluctuation variables

$$u(t, x, y, z) = U(t, x, y, z) - U^e(y) \quad (19)$$

$$p(t, x, y, z) = P(t, x, y, z) - P^e(y) \quad (20)$$

where $U^e(y)$ and $P^e(y)$ are, respectively, the equilibrium velocity and pressure given in Eqs. (15) and (17). The linearization of Eqs. (2)–(4) around the Hartmann equilibrium profile, written in the fluctuation variables (u, V, W, p, ϕ) , is

$$u_t = \frac{\Delta u}{\text{Re}} - U^e(y)u_x - U_y^e(y)V - p_x + N\phi_z - Nu \quad (21)$$

$$V_t = \frac{\Delta V}{\text{Re}} - U^e(y)V_x - p_y \quad (22)$$

$$W_t = \frac{\Delta W}{\text{Re}} - U^e(y)W_x - p_z - N\phi_x - NW \quad (23)$$

The equation for the potential is

$$\Delta \phi = u_z - W_x \quad (24)$$

and the fluctuation velocity field verifies the continuity equation

$$u_x + V_y + W_z = 0 \quad (25)$$

and the following boundary conditions:

$$u(t, x, 0, z) = W(t, x, 0, z) = V(t, x, 0, z) = 0 \quad (26)$$

$$u(t, x, 1, z) = U_c(t, x, z) \quad (27)$$

$$V(t, x, 1, z) = V_c(t, x, z) \quad (28)$$

$$W(t, x, 1, z) = W_c(t, x, z) \quad (29)$$

$$\phi(t, x, 0, z) = 0, \quad \phi(t, x, 1, z) = \Phi_c(t, x, z) \quad (30)$$

We denote the initial conditions for the fluctuation velocity as $u_0(x, y, z) = U_0(x, y, z) - U^e(y)$.

To guarantee stability, our design task is to design feedback laws U_c , V_c , W_c , and Φ_c so that the origin of the velocity fluctuation system is exponentially stable. Full-state knowledge is assumed.

Since the plant is linear and spatially invariant [34], we use a Fourier transform in the x and z coordinates (the spatially invariant directions). The transform pair (direct and inverse transform) is defined for any function $f(x, y, z)$ as

$$f(k_x, y, k_z) = \int_{-\infty}^{\infty} \int_{-\infty}^{\infty} f(x, y, z) e^{-2\pi i(k_x x + k_z z)} dz dx \quad (31)$$

$$f(x, y, z) = \int_{-\infty}^{\infty} \int_{-\infty}^{\infty} f(k_x, y, k_z) e^{2\pi i(k_x x + k_z z)} dk_z dk_x \quad (32)$$

Note that we use the same symbol f for both the original $f(x, y, z)$ and the image $f(k_x, y, k_z)$. In hydrodynamics k_x and k_z are referred to as the “wave numbers.”

The plant equations in wave number space are

$$u_t = \frac{-\alpha^2 u + u_{yy}}{\text{Re}} - \beta(y)u - U_y^e(y)V - 2\pi k_x i p - Nu + 2\pi k_z i N \phi \quad (33)$$

$$V_t = \frac{-\alpha^2 V + V_{yy}}{\text{Re}} - \beta(y)V - p_y \quad (34)$$

$$W_t = \frac{-\alpha^2 W + W_{yy}}{\text{Re}} - \beta(y)W - 2\pi k_z i p - NW - 2\pi k_x i N \phi \quad (35)$$

where $\alpha^2 = 4\pi^2(k_x^2 + k_z^2)$ and $\beta(y) = 2\pi i k_x U^e(y)$.

The continuity equation in wave number space is expressed as

$$2\pi i k_x u + V_y + 2\pi k_z W = 0 \quad (36)$$

and the equation for the potential is

$$-\alpha^2 \phi + \phi_{yy} = 2\pi i(k_z u - k_x W) \quad (37)$$

The boundary conditions are

$$u(t, k_x, 0, k_z) = W(t, k_x, 0, k_z) = V(t, k_x, 0, k_z) = 0 \quad (38)$$

$$u(t, k_x, 1, k_z) = U_c(t, k_x, k_z) \quad (39)$$

$$V(t, k_x, 1, k_z) = V_c(t, k_x, k_z) \quad (40)$$

$$W(t, k_x, 1, k_z) = W_c(t, k_x, k_z) \quad (41)$$

$$\phi(t, k_x, 0, k_z) = 0, \quad \phi(t, k_x, 1, k_z) = \Phi_c(t, k_x, k_z) \quad (42)$$

5 Control Design

We design the controller in wave number space. Note that Eqs. (33)–(42) are uncoupled for each wave number. It is well known that large wave numbers (which correspond to small scales where dissipation is present) are already stable, and instability can only be found in small wave numbers (large scale behavior) [3]. Therefore, as in Refs. [5,6], the set of wave numbers $k_x^2 + k_z^2 \leq M^2$, which we refer to as the *controlled* wave number range, and the set k_x^2

$+k_z^2 > M^2$, the *uncontrolled* wave number range, can be treated and studied separately. If stability for all wave numbers is established, stability in physical space follows (see Ref. [5]). The number M , which will be computed in Sec. 5.2, is a parameter that ensures stability for uncontrolled wave numbers.

We define χ , a *truncating* function, as

$$\chi(k_x, k_z) = \begin{cases} 1, & k_x^2 + k_z^2 \leq M^2 \\ 0 & \text{otherwise} \end{cases} \quad (43)$$

Then, we reflect that we do not use control for large wave numbers by setting

$$\begin{pmatrix} U_c(t, x, z) \\ V_c(t, x, z) \\ W_c(t, x, z) \\ \Phi_c(t, x, z) \end{pmatrix} = \int_{-\infty}^{\infty} \int_{-\infty}^{\infty} \begin{pmatrix} U_c(t, k_x, k_z) \\ V_c(t, k_x, k_z) \\ W_c(t, k_x, k_z) \\ \Phi_c(t, k_x, k_z) \end{pmatrix} \times \chi(k_x, k_z) e^{2\pi i(k_x x + k_z z)} dk_x dk_z \quad (44)$$

Next we design stabilizing control laws for small wave numbers and analyze uncontrolled wave numbers.

5.1 Controlled Wave Number Analysis. Consider $k_x^2 + k_z^2 \leq M^2$. Then $\chi=1$, so there is control. Using the continuity equation (36) and taking divergence of Eqs. (33)–(35), a Poisson equation for the pressure is derived,

$$-\alpha^2 p + p_{yy} = -4\pi k_x i U_y^e(y) V + N V_y \quad (45)$$

Evaluating Eq. (34) at $y=0$ one finds that

$$p_y(k_x, 0, k_z) = \frac{V_{yy}(k_x, 0, k_z)}{\text{Re}} = -2\pi i \frac{k_x u_{y0} + k_z W_{y0}}{\text{Re}} \quad (46)$$

where we use Eq. (36) for expressing V_{yy} at the bottom in terms of $u_{y0} = u_y(k_x, 0, k_z)$ and $W_{y0} = W_y(k_x, 0, k_z)$. Similarly, evaluating Eq. (34) at $y=1$ we get

$$\begin{aligned} p_y(k_x, 1, k_z) &= \frac{V_{yy}(k_x, 1, k_z)}{\text{Re}} - (V_c)_t - \alpha^2 \frac{V_c}{\text{Re}} = -2\pi i \frac{k_x u_{y1} + k_z W_{y1}}{\text{Re}} \\ &- (V_c)_t - \alpha^2 \frac{V_c}{\text{Re}} \end{aligned} \quad (47)$$

where we use Eq. (36) for expressing V_{yy} at the top wall in terms of $u_{y1} = u_y(k_x, 1, k_z)$ and $W_{y1} = W_y(k_x, 1, k_z)$ and the controller V_c .

Equation (45) can be solved in terms of integrals of the state and the boundary terms appearing in Eqs. (46) and (47).

$$\begin{aligned} p &= -\frac{4\pi k_x i}{\alpha} \int_0^y U_y^e(\eta) \sinh(\alpha(y-\eta)) V(k_x, \eta, k_z) d\eta \\ &+ N \int_0^y \frac{\sinh(\alpha(y-\eta))}{\alpha} V_y(k_x, \eta, k_z) d\eta \\ &+ 2\pi i \frac{\cosh(\alpha(1-y))}{\alpha \sinh \alpha} \frac{k_x u_{y0} + k_z W_{y0}}{\text{Re}} \\ &+ \frac{4\pi k_x i \cosh(\alpha y)}{\alpha \sinh \alpha} \int_0^1 U_y^e(\eta) \cosh(\alpha(1-\eta)) \times V(k_x, \eta, k_z) d\eta \\ &- N \frac{\cosh(\alpha y)}{\alpha \sinh \alpha} \int_0^1 \cosh(\alpha(1-\eta)) \times V_y(k_x, \eta, k_z) d\eta \\ &- 2\pi i \frac{\cosh(\alpha y)}{\alpha \sinh \alpha} \frac{k_x u_{y1} + k_z W_{y1}}{\text{Re}} - \frac{\cosh(\alpha y)}{\alpha \sinh \alpha} \left((V_c)_t + \alpha^2 \frac{V_c}{\text{Re}} \right) \end{aligned} \quad (48)$$

We proceed as in Refs. [5,6] and use the controller V_c , which appears *inside* the pressure solution (48), to make the pressure strict-feedback (spatially causal in y), which is a necessary struc-

ture for the application of a backstepping boundary controller [35]. Physically this means that we do not let pressure perturbations of the flow at one given point to be affected by the velocity field closer than the point to the upper wall; only the velocity field “below” the point (closer to the lower wall) can have any effect on the pressure perturbation.

Since the first three lines in Eq. (48) are already spatially causal, we need to cancel the fourth, fifth, and sixth lines of Eq. (48). Set

$$\begin{aligned} (V_c)_t &= \alpha^2 \frac{V_c}{\text{Re}} + 2\pi i \frac{k_x(u_{y0} - u_{y1}) + k_z(W_{y0} - W_{y1})}{\text{Re}} \\ &+ 4\pi k_x i \int_0^1 U_y^e(\eta) \cosh(\alpha(1-\eta)) V(k_x, \eta, k_z) d\eta \\ &- N \int_0^1 \cosh(\alpha(1-\eta)) V_y(k_x, \eta, k_z) d\eta \end{aligned} \quad (49)$$

which can be written as

$$\begin{aligned} (V_c)_t &= \alpha^2 \frac{V_c}{\text{Re}} + 2\pi i \frac{k_x(u_{y0} - u_{y1}) + k_z(W_{y0} - W_{y1})}{\text{Re}} - N V_c \\ &+ \int_0^1 \cosh(\alpha(1-\eta)) V(k_x, \eta, k_z) \times (N + 4\pi k_x i U_y^e(\eta)) d\eta \end{aligned} \quad (50)$$

Then, the pressure is written in terms of a strict-feedback integral of the state V and the boundary terms u_{y0} , W_{y0} (proportional to the skin friction at the bottom) as follows:

$$\begin{aligned} p &= -\frac{4\pi k_x i}{\alpha} \int_0^y U_y^e(\eta) \sinh(\alpha(y-\eta)) V(k_x, \eta, k_z) d\eta \\ &- 2\pi i \frac{\cosh(\alpha y) - \cosh(\alpha(1-y))}{\text{Re} \alpha \sinh \alpha} (k_x u_{y0} + k_z W_{y0}) \\ &+ N \int_0^y \frac{\sinh(\alpha(y-\eta))}{\alpha} V_y(k_x, \eta, k_z) d\eta \end{aligned} \quad (51)$$

Similarly, solving for ϕ in terms of the control Φ_c and the right hand side of its Poisson equation (37),

$$\begin{aligned} \phi &= \frac{2\pi i}{\alpha} \int_0^y \sinh(\alpha(y-\eta)) (k_z u(k_x, \eta, k_z) - k_x W(k_x, \eta, k_z)) d\eta \\ &+ \frac{\sinh(\alpha y)}{\sinh \alpha} \Phi_c(k_x, k_y) - \frac{2\pi i \sinh(\alpha y)}{\alpha \sinh \alpha} \int_0^1 \sinh(\alpha(1-\eta)) \\ &\times (k_z u(k_x, \eta, k_z) - k_x W(k_x, \eta, k_z)) d\eta \end{aligned} \quad (52)$$

As in the pressure, an actuator (Φ_c in this case) appears inside the solution for the potential. The last two lines of Eq. (52) are non-strict-feedback integrals and need to be canceled to apply the backstepping method. As for the pressure, this means that we do not let electric field perturbations of the flow at one given point to be affected by the velocity field further “up” than the point (closer to the upper wall); only the velocity field closer to the lower wall affects the electrical field perturbation.

For this we use Φ_c by setting

$$\Phi_c(k_x, k_y) = \frac{2\pi i}{\alpha} \int_0^1 \sinh(\alpha(1-\eta)) (k_z u(k_x, \eta, k_z) - k_x W(k_x, \eta, k_z)) d\eta \quad (53)$$

Then the potential can then be expressed as a strict-feedback integral of the states u and W as follows:

$$\phi = \frac{2\pi i}{\alpha} \int_0^y \sinh(\alpha(y-\eta))(k_z u(k_x, \eta, k_z) - k_x W(k_x, \eta, k_z)) d\eta \quad (54)$$

Introducing the expressions (51) and (54) in Eqs. (33) and (35), we get

$$\begin{aligned} u_t = & \frac{-\alpha^2 u + u_{yy}}{\text{Re}} - \beta(y)u - U_y^e(y)V - Nu - 4\pi^2 k_x \\ & \times \frac{\cosh(\alpha y) - \cosh(\alpha(1-y))}{\text{Re } \alpha \sinh \alpha} (k_x u_{y0} + k_z W_{y0}) \\ & - \frac{8\pi k_x^2}{\alpha} \int_0^y U_y^e(\eta) \sinh(\alpha(y-\eta)) V(k_x, \eta, k_z) d\eta \\ & - 2\pi i k_x N \int_0^y \frac{\sinh(\alpha(y-\eta))}{\alpha} V_y(k_x, \eta, k_z) d\eta \\ & - \frac{4\pi^2 k_x N}{\alpha} \int_0^y \sinh(\alpha(y-\eta)) \times (k_z U(k_x, \eta, k_z) \\ & - k_x W(k_x, \eta, k_z)) d\eta \end{aligned} \quad (55)$$

$$\begin{aligned} W_t = & \frac{-\alpha^2 W + W_{yy}}{\text{Re}} - \beta(y)W - NW - 4\pi^2 k_z \\ & \times \frac{\cosh(\alpha y) - \cosh(\alpha(1-y))}{\text{Re } \alpha \sinh \alpha} (k_x u_{y0} + k_z W_{y0}) \\ & - \frac{8\pi k_x k_z}{\alpha} \int_0^y U_y^e(\eta) \sinh(\alpha(y-\eta)) V(k_x, \eta, k_z) d\eta \\ & - 2\pi i k_z N \int_0^y \frac{\sinh(\alpha(y-\eta))}{\alpha} V_y(k_x, \eta, k_z) d\eta \\ & + \frac{4\pi^2 k_x N}{\alpha} \int_0^y \sinh(\alpha(y-\eta)) \times (k_z U(k_x, \eta, k_z) \\ & - k_x W(k_x, \eta, k_z)) d\eta \end{aligned} \quad (56)$$

We have omitted the equation for V since, from Eq. (36) and using the fact that $V(k_x, 0, k_z) = 0$, V is computed as

$$V = -2\pi i \int_0^y (k_x U(k_x, \eta, k_z) + k_z W(k_x, \eta, k_z)) d\eta \quad (57)$$

Now we use the following change in variables and its inverse:

$$Y = 2\pi i(k_x u + k_z W), \quad \omega = 2\pi i(k_z u - k_x W) \quad (58)$$

$$u = \frac{2\pi i}{\alpha^2}(k_x Y + k_z \omega), \quad W = \frac{2\pi i}{\alpha^2}(k_z Y - k_x \omega) \quad (59)$$

Note that ω is the normal vorticity, whereas $Y = -V_y$, the rate of change in the velocity V along the channel.

Defining $\epsilon = 1/\text{Re}$ and the following functions:

$$\begin{aligned} g_1 = & 4\pi i k_x \left\{ \frac{U_y^e(y)}{2} + \int_\eta^y U_y^e(\sigma) \frac{\sinh(\alpha(y-\sigma))}{\alpha} d\sigma \right\} \\ & + N\alpha \sinh(\alpha(y-\sigma)) \end{aligned} \quad (60)$$

$$g_2 = -\alpha \frac{\cosh(\alpha y) - \cosh(\alpha(1-y))}{\text{Re } \sinh \alpha} \quad (61)$$

$$h_1 = 2\pi i k_z U_y^e \quad (62)$$

$$h_2 = -N\alpha \sinh(\alpha(y-\eta)) \quad (63)$$

Eqs. (55) and (56) expressed in terms of Y and ω are

$$\begin{aligned} Y_t = & \epsilon(-\alpha^2 Y + Y_{yy}) - \beta(y)Y - NY + gY_{y0} \\ & + \int_0^y f(k_x, y, \eta, k_z) Y(k_x, \eta, k_z) d\eta \end{aligned} \quad (64)$$

$$\begin{aligned} \omega_t = & \epsilon(-\alpha^2 \omega + \omega_{yy}) - \beta(y)\omega - N\omega + h_1(y) \int_0^y Y(k_x, \eta, k_z) d\eta \\ & + \int_0^y h_2(y, \eta) \omega(k_x, \eta, k_z) d\eta \end{aligned} \quad (65)$$

where we have used the inverse change in variables (59) to express u_{y0} and W_{y0} in terms of $Y_{y0} = Y_y(k_x, 0, k_z)$ as follows:

$$Y_{y0} = 2\pi i(k_x u_{y0} + k_z W_{y0}) \quad (66)$$

with boundary conditions

$$Y(t, k_x, 0, k_z) = \omega(t, k_x, 0, k_z) = 0 \quad (67)$$

$$Y(t, k_x, 1, k_z) = Y_c(t, k_x, k_z) \quad (68)$$

$$\omega(t, k_x, 1, k_z) = \omega_c(t, k_x, k_z) \quad (69)$$

where

$$Y_c = 2\pi i(k_x U_c + k_z W_c) \quad (70)$$

$$\omega_c = 2\pi i(k_z U_c - k_x W_c) \quad (71)$$

Equations (64) and (65) are a coupled, strict-feedback plant, with integral and reaction terms. As in Ref. [6], a variant of the design presented in Ref. [35] can be used to stabilize the system using a double backstepping transformation. The transformation maps, for each k_x and k_z , the variables (Y, ω) into the variables (Ψ, Ω) , verify the following family of heat equations (parametrized in k_x, k_z):

$$\Psi_t = \epsilon(-\alpha^2 \Psi + \Psi_{yy}) - \beta(y)\Psi - N\Psi \quad (72)$$

$$\Omega_t = \epsilon(-\alpha^2 \Omega + \Omega_{yy}) - \beta(y)\Omega - N\Omega \quad (73)$$

with boundary conditions

$$\Psi(k_x, 0, k_z) = \Psi(k_x, 1, k_z) = 0 \quad (74)$$

$$\Omega(k_x, 0, k_z) = \Omega(k_x, 1, k_z) = 0 \quad (75)$$

The transformation is defined as follows:

$$\Psi = Y - \int_0^y K(k_x, y, \eta, k_z) Y(k_x, \eta, k_z) d\eta \quad (76)$$

$$\begin{aligned} \Omega = & \omega - \int_0^y \Gamma_1(k_x, y, \eta, k_z) Y(k_x, \eta, k_z) d\eta \\ & - \int_0^y \Gamma_2(k_x, y, \eta, k_z) \omega(k_x, \eta, k_z) d\eta \end{aligned} \quad (77)$$

Following Refs. [35,5,6], the functions $K(k_x, y, \eta, k_z)$, $\Gamma_1(k_x, y, \eta, k_z)$, and $\Gamma_2(k_x, y, \eta, k_z)$ are found as the solution of the following partial integrodifferential equations:

$$\epsilon K_{yy} = \epsilon K_{\eta\eta} + (\beta(y) - \beta(\eta))K - f + \int_\eta^y f(\eta, \xi) K(y, \xi) d\xi \quad (78)$$

$$\begin{aligned} \epsilon \Gamma_{1yy} = & \epsilon \Gamma_{1\eta\eta} + (\beta(y) - \beta(\eta))\Gamma_1 - h_1 + \int_{\eta}^y \Gamma_2(y, \xi) \times h_1(\xi) d\xi \\ & + \int_{\eta}^y f(\eta, \xi)\Gamma_1(y, \xi) d\xi \end{aligned} \quad (79)$$

$$\epsilon \Gamma_{2yy} = \epsilon \Gamma_{2\eta\eta} + (\beta(y) - \beta(\eta))\Gamma_2 - h_2 + \int_{\eta}^y h_2(\xi, \eta)\Gamma_2(y, \xi) d\xi \quad (80)$$

Equations (78)–(80) are hyperbolic partial integrodifferential equations in the region $\mathcal{T} = \{(y, \eta) : 0 \leq y \leq 1, 0 \leq \eta \leq y\}$. Their boundary conditions are

$$K(y, y) = -\frac{g(0)}{\epsilon} \quad (81)$$

$$K(y, 0) = \frac{\int_0^y K(y, \eta)g(\eta) d\eta - g(y)}{\epsilon} \quad (82)$$

$$\Gamma_1(y, 0) = \frac{\int_0^y \Gamma_1(y, \eta)g(\eta) d\eta}{\epsilon} \quad (83)$$

$$\Gamma_1(y, y) = 0, \Gamma_2(y, y) = 0, \Gamma_2(y, 0) = 0 \quad (84)$$

Remark 5.1. Equations (78)–(84) are well posed and can be solved symbolically, by means of a successive approximation series, or numerically [35,6]. Note that Eqs. (78) and (80) are autonomous. Hence, one must solve first for $K(k_x, y, \eta, k_z)$ and $\Gamma_2(k_x, y, \eta, k_z)$. Then the solution for Γ_2 is plugged in Eq. (79), which then can be solved for $\Gamma_1(k_x, y, \eta, k_z)$.

Control laws Y_c and W_c are found by evaluating Eqs. (76) and (77) at $y=1$ and using Eqs. (68), (69), (74), and (75), which yields

$$Y_c(t, k_x, k_z) = \int_0^1 K(k_x, 1, \eta, k_z) Y(k_x, \eta, k_z) d\eta \quad (85)$$

$$\begin{aligned} \omega_c(t, k_x, k_z) = & \int_0^1 \Gamma_1(k_x, 1, \eta, k_z) Y(k_x, \eta, k_z) d\eta \\ & + \int_0^1 \Gamma_2(k_x, 1, \eta, k_z) \omega(k_x, \eta, k_z) d\eta \end{aligned} \quad (86)$$

Using Eqs. (58) and (59) to write Eqs. (85) and (86) in (u, W) , we get

$$\begin{aligned} U_c = & \int_0^1 K^{Uu}(k_x, 1, \eta, k_z) u(k_x, \eta, k_z) d\eta \\ & + \int_0^1 K^{UW}(k_x, 1, \eta, k_z) W(k_x, \eta, k_z) d\eta \end{aligned} \quad (87)$$

$$\begin{aligned} W_c = & \int_0^1 K^{Wu}(k_x, 1, \eta, k_z) u(k_x, \eta, k_z) d\eta \\ & + \int_0^1 K^{WW}(k_x, 1, \eta, k_z) W(k_x, \eta, k_z) d\eta \end{aligned} \quad (88)$$

where

$$\begin{pmatrix} K^{Uu} \\ K^{UW} \\ K^{Wu} \\ K^{WW} \end{pmatrix} = \mathbf{A} \begin{pmatrix} K(k_x, y, \eta, k_z) \\ \Gamma_1(k_x, y, \eta, k_z) \\ 0 \\ \Gamma_2(k_x, y, \eta, k_z) \end{pmatrix} \quad (89)$$

and where the matrix \mathbf{A} is defined as

$$\mathbf{A} = -\frac{4\pi^2}{\alpha^2} \begin{pmatrix} k_x^2 & k_x k_z & k_x k_z & k_z^2 \\ k_x k_z & k_z^2 & -k_x^2 & -k_x k_z \\ k_x k_z & -k_x^2 & k_z^2 & -k_x k_z \\ k_z^2 & -k_x k_z & -k_x k_z & k_x^2 \end{pmatrix} \quad (90)$$

Stability in the controlled wave number range follows from stability of Eqs. (72) and (73) and the invertibility of the transformations (76) and (77). We get the following result, whose proof we sketch (see Ref. [6] for more details).

PROPOSITION 5.1. For $k_x^2 + k_z^2 \leq M^2$, the equilibrium $u \equiv V \equiv W \equiv 0$ of systems (33)–(42) with control laws (50), (53), (87), and (88) is exponentially stable in the L^2 norm, i.e.,

$$\begin{aligned} \int_0^1 (|u|^2 + |V|^2 + |W|^2)(t, k_x, y, k_z) dy \leq & C_1 e^{-2\epsilon t} \int_0^1 (|u_0|^2 + |V_0|^2 \\ & + |W_0|^2)(0, k_x, y, k_z) dy \end{aligned} \quad (91)$$

where $C_1 \geq 0$.

Proof. From Eqs. (72) and (73) we get, using a standard Lyapunov argument,

$$\int_0^1 (|\Psi|^2 + |\Omega|^2)(t, k_x, y, k_z) dy \leq e^{-2\epsilon t} \int_0^1 (|\Psi|^2 + |\Omega|^2)(0, k_x, y, k_z) dy \quad (92)$$

and then from the transformations (76) and (77) and its inverse (which is guaranteed to exist [35]), we get

$$\begin{aligned} \int_0^1 (|Y|^2 + |\omega|^2)(t, k_x, y, k_z) dy \leq & C_0 e^{-2\epsilon t} \int_0^1 (|Y|^2 + |\omega|^2) \\ & \times (0, k_x, y, k_z) dy \end{aligned} \quad (93)$$

where $C_0 > 0$ is a constant depending on the kernels K , Γ_1 and Γ_2 , and their inverses. Then writing (u, W) in terms of (Y, ω) and bounding the norm of V by the norm of Y (using $Y = -V_y$ and Poincaré's inequality), the result follows. \square

5.2 Uncontrolled Wave Number Analysis. When $k_x^2 + k_z^2 > M$, the plant verifies the following equations:

$$u_t = \frac{-\alpha^2 u + u_{yy}}{\text{Re}} - \beta(y)u - U_y^e(y)V - 2\pi k_x i p + 2\pi k_z i N \phi - Nu \quad (94)$$

$$V_t = \frac{-\alpha^2 V + V_{yy}}{\text{Re}} - \beta(y)V - p_y \quad (95)$$

$$W_t = \frac{-\alpha^2 W + W_{yy}}{\text{Re}} - \phi W - 2\pi k_z i p - 2\pi k_x i N \phi - NW \quad (96)$$

the Poisson equation for the potential

$$-\alpha^2 \phi + \phi_{yy} = 2\pi i (k_z u - k_x W) \quad (97)$$

the continuity equation

$$2\pi i k_x u + V_y + 2\pi k_z W = 0 \quad (98)$$

and Dirichlet boundary conditions

$$u(t, k_x, 0, k_y) = V(t, k_x, 0, k_y) = W(t, k_x, 0, k_y) = 0 \quad (99)$$

$$u(t, k_x, 1, k_y) = V(t, k_x, 1, k_y) = W(t, k_x, 1, k_y) = 0 \quad (100)$$

$$\phi(t, k_x, 0, k_y) = \phi(t, k_x, 1, k_y) = 0 \quad (101)$$

Using Eq. (58), one gets the following equations for Y and ω :

$$Y_t = \epsilon(-\alpha^2 Y + Y_{yy}) - \beta(y)Y - 2\pi k_x i U_y^e(y)V + \alpha^2 p - NY \quad (102)$$

$$\omega_t = \epsilon(-\alpha^2 \omega + \omega_{yy}) - \beta(y)\omega - 2\pi k_x i U_y^e(y)V - \alpha^2 N\phi - N\omega \quad (103)$$

The Poisson equation for the potential is, in terms of ω ,

$$-\alpha^2 \phi + \phi_{yy} = \omega \quad (104)$$

Consider the Lyapunov function

$$\Lambda = \int_0^1 \frac{|u|^2 + |V|^2 + |W|^2}{2} dy \quad (105)$$

where we write $\int_0^1 f = \int_0^1 f(k_x, y, k_z) dy$. The function Λ is the L^2 norm (kinetic energy) of the perturbation velocity field (which is closely related to the turbulent kinetic energy).

Denote by f^* the complex conjugate of f . Substituting Y and ω from Eq. (59) into Eq. (105), we get

$$\begin{aligned} \Lambda &= \int_0^1 4\pi^2 \left[\frac{k_x^2 |Y|^2 + k_z^2 |\omega|^2 + k_x k_z (Y^* \omega + Y \omega^*) + k_z^2 |Y|^2}{2\alpha^4} \right. \\ &\quad \left. + \frac{k_x^2 |\omega|^2 - k_x k_z (Y^* \omega + Y \omega^*)}{2\alpha^4} \right] + \int_0^1 \frac{|V|^2}{2} \\ &= \int_0^1 \frac{|Y|^2 + |\omega|^2 + \alpha^2 |V|^2}{2\alpha^2} \end{aligned} \quad (106)$$

Define then a new Lyapunov function

$$\Lambda_1 = \alpha^2 \Lambda = \int_0^1 \frac{|Y|^2 + |\omega|^2 + \alpha^2 |V|^2}{2} \quad (107)$$

The time derivative of Λ_1 can be estimated as follows:

$$\begin{aligned} \dot{\Lambda}_1 &= -2\epsilon\alpha^2 \Lambda_1 - \epsilon \int_0^1 (|Y_y|^2 + |\omega_y|^2 + \alpha^2 |V_y|^2) - N \int_0^1 (|Y|^2 + |\omega|^2) \\ &\quad - \alpha^2 N \int_0^1 \frac{\phi^* \omega + \phi \omega^*}{2} + \int_0^1 \pi i U_y^e(y) [V^* (2k_x Y + k_z \omega) \\ &\quad - V (2k_x Y^* + k_z \omega^*)] + \alpha^2 \int_0^1 \frac{P^* Y + P Y^* - P_y^* V - P_y V^*}{2} \end{aligned} \quad (108)$$

For bounding (108), we use the following two lemmas.

LEMMA 5.1. $-\alpha^2 \int_0^1 \phi^* \omega + \phi \omega^* / 2 \leq \int_0^1 |\omega|^2$.

Proof. The term we want to estimate is

$$-\alpha^2 \int_0^1 \frac{\phi^* \omega + \phi \omega^*}{2} \quad (109)$$

Substituting $\alpha^2 \phi$ from Eq. (104), Eq. (109) can be written as

$$-\int_0^1 \frac{\phi_{yy}^* \omega + \phi_{yy} \omega^*}{2} + \int_0^1 |\omega|^2 \quad (110)$$

Therefore, we need to prove that

$$\int_0^1 (\phi_{yy}^* \omega + \phi_{yy} \omega^*) \geq 0 \quad (111)$$

Substituting ω from Eq. (104) into Eq. (111), we get

$$\begin{aligned} \int_0^1 (\phi_{yy}^* \omega + \phi_{yy} \omega^*) &= \int_0^1 |\phi_{yy}|^2 - \alpha^2 \int_0^1 (\phi_{yy}^* \phi + \phi_{yy} \phi^*) \\ &= \int_0^1 |\phi_{yy}|^2 + \alpha^2 \int_0^1 |\phi_y|^2 \end{aligned} \quad (112)$$

which is non-negative. \square

LEMMA 5.2. $|U_y^e(y)| \leq 4 + H$.

Proof. Computing $U_y^e(y)$ from Eq. (15),

$$U_y^e(y) = H \frac{\cosh(Hy) - \cosh(H(1-y))}{2 \sinh H/2 - \sinh H} \quad (113)$$

Calling $g_1(y) = \cosh(Hy) - \cosh(H(1-y))$, since $g_1'(y) = H(\sinh(Hy) + \sinh(H(1-y)))$ is always positive for $y \in (0, 1)$, the maximum must be in the boundaries. Therefore

$$|U_y^e(y)| \leq g_2(H) = H \frac{\cosh H - 1}{\sinh H - 2 \sinh H/2} \quad (114)$$

One can rewrite g_2 as

$$g_2 = H \frac{\sinh H/2}{\cosh H/2 - 1} \quad (115)$$

Since $g_2(0) = 4$, it suffices to verify that $g_2'(H) \leq 1$.

$$g_2'(H) = \frac{g_3}{g_4} = \frac{\sinh H/2 - H^2/2}{\cosh H/2 - 1} \quad (116)$$

This is equivalent to verify that $g_3 \leq g_4$. Since $g_3(0) = g_4(0) = 0$, it is enough that $g_3' \leq g_4'$, which follows from

$$g_3' = H/2(\cosh H/2 - 2H) \leq H/2(\sinh H/2) = g_4' \quad (117)$$

because $\cosh x - 4x \leq \sinh x$. \square

Integrating by parts and applying Lemma 1,

$$\begin{aligned} \dot{\Lambda}_1 &\leq -2\epsilon\alpha^2 \Lambda_1 - \epsilon \int_0^1 (|Y_y|^2 + |\omega_y|^2 + \alpha^2 |V_y|^2) \\ &\quad + \int_0^1 \pi i U_y^e(y) V^* (k_x Y + k_z \omega) - \int_0^1 \pi i U_y^e(y) V (k_x Y^* + k_z \omega^*) \\ &\quad - N \int_0^1 |Y|^2 \end{aligned} \quad (118)$$

Using Lemma 2 to bound U_y^e in Eq. (118),

$$\begin{aligned} \dot{\Lambda}_1 &\leq -2\epsilon(1 + \alpha^2)\Lambda_1 - N \int_0^1 |Y|^2 dy + 2\pi(4 + H) \int_0^1 (|V|(|k_x| |Y| \\ &\quad + |k_z| |\omega|) dy \leq (4 + H - 2\epsilon(1 + \alpha^2))\Lambda_1 \end{aligned} \quad (119)$$

where we have applied Young's and Poincaré's inequalities. Hence, if $\alpha^2 \geq (4 + H)/2\epsilon$,

$$\dot{\Lambda}_1 \leq -2\epsilon\Lambda_1 \quad (120)$$

Dividing Eq. (120) by α^2 and using Eq. (107), we get

$$\dot{\Lambda} \leq -2\epsilon\Lambda \quad (121)$$

and stability in the uncontrolled wave number range follows when $k_x^2 + k_z^2 \geq M^2$ for M (conservatively) chosen as

$$M \geq \frac{1}{2\pi} \sqrt{\frac{(H+4)\text{Re}}{2}} \quad (122)$$

We summarize the result in the following proposition.

PROPOSITION 5.2. For $k_x^2 + k_z^2 \geq M^2$, where $M \geq 1/2\pi\sqrt{(H+4)\text{Re}/2}$, the equilibrium $u \equiv V \equiv W \equiv 0$ of the un-

controlled systems (94)–(101) is exponentially stable in the L^2 sense, i.e.,

$$\int_0^1 (|u|^2 + |V|^2 + |W|^2)(t, k_x, y, k_z) dy + \leq e^{-2\epsilon t} \int_0^1 (|u_0|^2 + |V_0|^2 + |W_0|^2)(k_x, y, k_z) dy \quad (123)$$

5.3 Main Result. Substituting Eqs. (50), (53), (87), and (88) into Eq. (44), and using the Fourier convolution theorem, we get the control laws in physical space, which can be expressed compactly as

$$\begin{pmatrix} U_c \\ W_c \\ \Phi_c \end{pmatrix} = \int_{-\infty}^{\infty} \int_0^1 \int_{-\infty}^{\infty} \Sigma(x - \xi, \eta, z - \zeta) \times \begin{pmatrix} u(\xi, \eta, \zeta) \\ W(\xi, \eta, \zeta) \end{pmatrix} d\xi d\eta d\zeta \quad (124)$$

where

$$\Sigma(\xi, \eta, \zeta) = \int_{-\infty}^{\infty} \int_{-\infty}^{\infty} \Sigma(k_x, \eta, k_z) \times \chi(k_x, k_z) e^{2\pi i(k_x \xi + k_z \zeta)} dk_z dk_x \quad (125)$$

and

$$\Sigma = \begin{pmatrix} K^{Uu}(k_x, 1, \eta, k_z) & K^{UW}(k_x, 1, \eta, k_z) \\ K^{Wu}(k_x, 1, \eta, k_z) & K^{WW}(k_x, 1, \eta, k_z) \\ \frac{2\pi i k_z}{\alpha} \sinh(\alpha(1 - \eta)) & -\frac{2\pi i k_x}{\alpha} \sinh(\alpha(1 - \eta)) \end{pmatrix} \quad (126)$$

Control law V_c is a dynamic feedback law computed as the solution of the following forced parabolic equation:

$$(V_c)_t = \frac{(V_c)_{xx} + (V_c)_{zz}}{\text{Re}} - NV_c + g(t, x, z) \quad (127)$$

where $g(t, x, z)$ is defined as

$$g = \int_{-\infty}^{\infty} \int_{-\infty}^{\infty} \left[\int_0^1 g_V(x - \xi, \eta, z - \zeta) V(\xi, \eta, \zeta) d\eta + g_W(x - \xi, z - \zeta) \times (W_y(\xi, 0, \zeta) - W_y(\xi, 1, \zeta)) + g_u(x - \xi, z - \zeta) (u_y(\xi, 0, \zeta) - u_y(\xi, 1, \zeta)) \right] d\xi d\zeta \quad (128)$$

and

$$g_u = \int_{-\infty}^{\infty} \int_{-\infty}^{\infty} 2\pi i \frac{k_x}{\text{Re}} \chi(k_x, k_z) e^{2\pi i(k_x \xi + k_z \zeta)} dk_z dk_x \quad (129)$$

$$g_V = \int_{-\infty}^{\infty} \int_{-\infty}^{\infty} \cosh(\alpha(1 - \eta)) (N + 4\pi k_x i U_y^e(\eta)) \times \chi(k_x, k_z) e^{2\pi i(k_x \xi + k_z \zeta)} dk_z dk_x \quad (130)$$

$$g_W = \int_{-\infty}^{\infty} \int_{-\infty}^{\infty} 2\pi i \frac{k_z}{\text{Re}} \chi(k_x, k_z) e^{2\pi i(k_x \xi + k_z \zeta)} dk_z dk_x \quad (131)$$

As in Refs. [5,6], considering all wave numbers and using Propositions 1 and 2, the following result holds regarding the convergence of the closed-loop system.

THEOREM 1. Consider the systems (21)–(30) with control laws (124)–(131). Then the equilibrium profile $u \equiv V \equiv W \equiv 0$ is asymptotically stable in the L^2 norm, i.e.,

$$\int_{-\infty}^{\infty} \int_0^1 \int_{-\infty}^{\infty} (u^2 + V^2 + W^2)(t) dx dy dz \leq C_2 e^{-2\epsilon t} \int_{-\infty}^{\infty} \int_0^1 \int_{-\infty}^{\infty} (u_0^2 + V_0^2 + W_0^2)(x, y, z) dx dy dz \quad (132)$$

where $C_2 = \max\{C_1, 1\} \geq 0$.

We have assumed in the above result that the closed-loop linearized system is well posed and that the velocity and electromagnetic field equations have at least L^2 solutions. See Ref. [40] for some mathematical considerations on the well-posedness of MHD problems.

Remark 5.2. In case that $N=0$, meaning that either there is no imposed magnetic field or the fluid is nonconducting, Eqs. (2)–(4) are the Navier–Stokes equations. Some physical insight can be gained by analyzing this case. In the context of hydrodynamics stability theory, the linearized observer error systems written in (Y, ω) variables verify equations analogous to the classical Orr–Sommerfeld–Squire equations. These are Eqs. (64) and (65) for controlled wave numbers and Eqs. (102) and (103) for uncontrolled wave numbers. As in Ref. [6], we use the backstepping transformations (76) and (77) not only to stabilize (damping the system using gain l) but also to decouple the system (using gains Γ_1, Γ_2) in the small wave number range, where non-normality effects are more severe. Even if the linearized system is stable, non-normality produces large transient growths [3,37], which enhanced by nonlinear effects may allow the system to go far away from the origin, activating the mechanism of transition to turbulence. This warrants the use of extra gains to map the system into two uncoupled heat equations (72) and (73).

Remark 5.3. As in Ref. [5], Theorem 2, some properties of the feedback control laws can be derived. The most important properties of the feedback laws from the point of view of implementation are the spatial decay of the kernels and conservation of mass. Spatial decay means that the function $\Sigma(x, y, z)$ appearing in Eq. (124) rapidly decreases as x or z grows and that implies that the control law mostly needs information about the states close to the actuation point. This suggests that our control laws could be approximately implemented by an array of discrete actuators, each of them only requiring information from the flow in its vicinity. Conservation of mass is derived by studying the behavior of the control laws at wave numbers $k_x = k_z = 0$ and can be mathematically expressed as

$$\int_{-\infty}^{\infty} \int_{-\infty}^{\infty} V_c(x, z) dx dz = 0 \quad (133)$$

Physically, it means that the actuators do not need to add or subtract mass from the flow to stabilize it, which is a very desirable property for a possible implementation.

6 Concluding Remarks

In this paper we have stabilized the Hartmann flow, a benchmark MHD model with several potential applications. We have used the backstepping method that allows to compute the control kernels without needing to discretize the system. Our solution is summarized in control laws (124)–(131) and Theorem 1. The feedback kernels given by Eqs. (89) and (90) and calculated from Eqs. (78)–(84) can be computed beforehand.

The design of the control laws (124)–(131) was based on using several invertible transformations to simplify the problem and then go back to obtain the solution in physical space. Figure 3 summarizes all the transformations that were used. The structure of the controller is shown in Fig. 4 (top).

These feedback laws require full-state knowledge. In Ref. [32] we presented an observer for estimation of velocity and electromagnetic fields of the Hartmann flow based on boundary measurements of pressure, current, and skin friction. Such an observer can be used together with the control laws (124)–(131) to obtain an output feedback stabilizing boundary controller that only needs

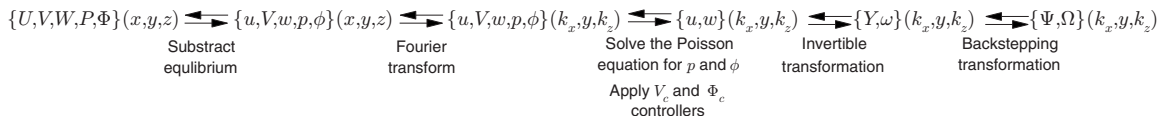


Fig. 3 The chain of transformations used to design the control laws. Note that all transformations are invertible.

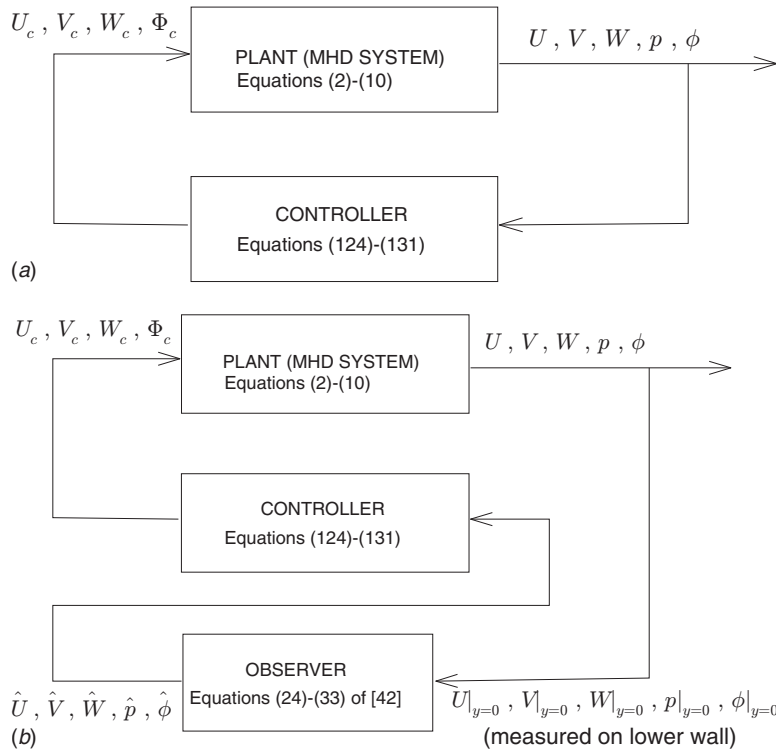


Fig. 4 A block diagram showing the structure of the controller. (Top) Full-state controller. (Bottom) Output-feedback controller (with measurements on the lower wall).

boundary measurements; a block diagram showing the structure of the proposed output feedback controller is shown in Fig. 4 (bottom).

This work can be used as the starting point to also solve the problems of motion planning and trajectory tracking, which are of interest in engineering applications. The problem has been solved in the case of nonconducting fluids [41] using the backstepping method.

Our result uses the *linear* backstepping control method for parabolic PDEs and thus requires linearization of the MHD equations as a first step. Hence, Theorem 1 only holds for initial conditions close enough to the equilibrium profile. If one considers instead the fully nonlinear MHD equations, the problem is extremely challenging not only because of the nonlinearity itself but also because the plant becomes coupled in the wave number space. The nonlinearity is of bilinear type, and recent developments that extend the backstepping method to nonlinear parabolic PDEs using Volterra series [42,43] and to the viscous Burgers equation [44,45] are potentially applicable; however, the method has to be extended to consider the coupling between different wave numbers.

Nomenclature

- j = electric current
- k_x, k_y = wave numbers
- K, Γ_1, Γ_2 = control kernels
- H = Hartmann number

- N = Stuart number
- P = pressure
- p = pressure fluctuation
- Re = Reynolds number
- Re_M = magnetic Reynolds number
- U = streamwise velocity
- U^e = streamwise equilibrium velocity
- U_c = streamwise velocity controller
- u = streamwise velocity fluctuation
- V = wall-normal velocity
- V_c = wall-normal velocity controller
- W = spanwise velocity
- W_c = spanwise velocity controller
- ϕ = electric potential
- Φ_c = electric potential controller
- Λ = Lyapunov function

References

- [1] Hartmann, J., 1937, "Theory of the Laminar Flow of an Electrically Conductive Liquid in a Homogeneous Magnetic Field," *K. Dan. Vidensk. Selsk. Mat. Fys. Medd.*, **15**(6), pp. 1–27.
- [2] Muller, U., and Buhler, L., 2001, *Magneto-fluidynamics in Channels and Containers*, Springer, Berlin.
- [3] Schmid, P. J., and Henningson, D. S., 2001, *Stability and Transition in Shear Flows*, Springer, New York.
- [4] Högberg, M., Bewley, T. R., and Henningson, D. S., 2003, "Linear Feedback Control and Estimation of Transition in Plane Channel Flow," *J. Fluid Mech.*, **481**, pp. 149–175.
- [5] Vazquez, R., and Krstic, M., 2007, "A Closed-Form Feedback Controller for

- Stabilization of the Linearized 2D Navier-Stokes Poiseuille Flow," IEEE Trans. Autom. Control, **52**, pp. 2298–2312.
- [6] Cochran, J., Vazquez, R., and Krstic, M., 2006, "Backstepping Boundary Control of Navier-Stokes Channel Flow: A 3D Extension," *Proceedings of the 2006 American Control Conference*.
- [7] Triggiani, R., 2007, "Stability Enhancement of a 2-D Linear Navier-Stokes Channel Flow by a 2-D, Wall-Normal Boundary Controller," *Discrete Contin. Dyn. Syst., Ser. B*, **8**(2), pp. 279–314.
- [8] Aamo, O. M., and Krstic, M., 2002, *Flow Control by Feedback: Stabilization and Mixing*, Springer, New York.
- [9] Balogh, A., Liu, W.-J., and Krstic, M., 2001, "Stability Enhancement by Boundary Control in 2D Channel Flow," IEEE Trans. Autom. Control, **46**, pp. 1696–1711.
- [10] Baker, J., Armaou, A., and Christofides, P., 2000, "Nonlinear Control of Incompressible Fluid Flow: Application to Burgers' Equation and 2D Channel Flow," *J. Math. Anal. Appl.*, **252**, pp. 230–255.
- [11] Vladimirov, V., and Ilin, K., 1998, "The Three-Dimensional Stability of Steady MHD Flows of an Ideal Fluid," *Phys. Plasmas*, **5**(12), pp. 4199–4204.
- [12] Takashima, M., 1996, "The Stability of the Modified Plane Poiseuille Flow in the Presence of a Transverse Magnetic Field," *Fluid Dyn. Res.*, **17**, pp. 293–310.
- [13] Krasnov, D., Zienicke, E., Zikanov, O., Boeck, T., and Thess, A., 2004, "Numerical Study of the Instability of the Hartmann Layer," *J. Fluid Mech.*, **504**, pp. 183–211.
- [14] Lock, R., 1955, "The Stability of the Flow of an Electrically Conducting Fluid Between Parallel Planes Under a Transverse Magnetic Field," *Proc. R. Soc. London, Ser. A*, **233**, pp. 105–125.
- [15] Albrecht, T., Metzkes, H., Grundmann, R., Mutschke, G., and Gerbeth, G., 2008, "Tollmien-Schlichting Wave Damping by a Streamwise Oscillating Lorentz Force," *Magnetohydrodynamics*, **44**(3), pp. 205–222.
- [16] Pang, J., and Choi, K.-S., 2004, "Turbulent Drag Reduction by Lorentz Force Oscillation," *Phys. Fluids*, **16**(5), pp. L35–L38.
- [17] Breuer, K., Park, J., and Henocho, C., 2004, "Actuation and Control of a Turbulent Channel Flow Using Lorentz Forces," *Phys. Fluids*, **16**(4), pp. 897–907.
- [18] Spong, E., Reizes, J., and Leonardi, E., 2005, "Efficiency Improvements of Electromagnetic Flow Control," *Int. J. Heat Fluid Flow*, **26**, pp. 635–655.
- [19] Berger, W., Kim, J., Lee, C., and Lim, J., 2000, "Turbulent Boundary Layer Control Utilizing the Lorentz Force," *Phys. Fluids*, **12**, pp. 631–649.
- [20] Choi, H., Moin, P., and Kim, J., 1994, "Active Turbulence Control for Drag Reduction in Wall-Bounded Flows," *J. Fluid Mech.*, **262**, pp. 75–110.
- [21] Baker, J., and Christofides, P., 2002, "Drag Reduction in Transitional Linearized Channel Flow Using Distributed Control," *Int. J. Control*, **75**, pp. 1213–1218.
- [22] Airiau, C., and Castets, M., 2004, "On the Amplification of Small Disturbances in a Channel Flow With a Normal Magnetic Field," *Phys. Fluids*, **16**, pp. 2991–3005.
- [23] Debbagh, K., Cathalifaud, P., and Airiau, C., 2007, "Optimal and Robust Control of Small Disturbances in a Channel Flow With a Normal Magnetic Field," *Phys. Fluids*, **19**(1), p. 014103.
- [24] Thibault, J.-P., and Rossi, L., 2003, "Electromagnetic Flow Control: Characteristic Numbers and Flow Regimes of a Wall-Normal Actuator," *J. Phys. D: Appl. Phys.*, **36**, pp. 2559–2568.
- [25] Singh, S., and Bandyopadhyay, P., 1997, "Linear Feedback Control of Boundary Layer Using Electromagnetic Microtiles," *ASME J. Fluids Eng.*, **119**(4), pp. 852–858.
- [26] Barbu, V., Popa, C., Havarneanu, T., and Sritharan, S., 2003, "Exact Controllability of Magneto-Hydrodynamic Equations," *Commun. Pure Appl. Math.*, **56**(6), pp. 732–783.
- [27] Sritharan, S., Barbu, V., Havarneanu, T., and Popa, C., 2005, "Advances in Differential Equations," *IEEE Trans. Autom. Control*, **10**(5), pp. 481–504.
- [28] Dietiker, J.-F., and Hoffmann, K., 2002, "Backstepping Boundary Control of Navier-Stokes Channel Flow: A 3D Extension," *AIAA Paper No. 2002-0130*.
- [29] Schuster, E., and Krstic, M., 2003, "Inverse Optimal Boundary Control for Mixing in Magnetohydrodynamic Channel Flows," *Proceedings of the 2003 CDC*.
- [30] Schuster, E., Luo, L., and Krstic, M., 2008, "MHD Channel Flow Control in 2D: Mixing Enhancement by Boundary Feedback," *Automatica*, **44**, pp. 2498–2507.
- [31] Bandyopadhyay, P. R., and Castano, J. M., 1996, "Micro-Tiles for Electromagnetic Turbulence Control in Saltwater—Preliminary Investigations," *ASME Fluids Engineering Division Conference, Vol. 2*, p. 53.
- [32] Vazquez, R., Schuster, E., and Krstic, M., 2008, "Magnetohydrodynamic State Estimation With Boundary Sensors," *Automatica*, **44**, pp. 2517–2527.
- [33] Xu, C., Schuster, E., Vazquez, R., and Krstic, M., 2008, "Stabilization of Linearized 2D Magnetohydrodynamic Channel Flow by Backstepping Boundary Control," *Syst. Control Lett.*, **57**, pp. 805–812.
- [34] Bamieh, B., Paganini, F., and Dahleh, M. A., 2000, "Distributed Control of Spatially-Invariant Systems," *IEEE Trans. Autom. Control*, **45**, pp. 1091–1107.
- [35] Smyshlyaev, A., and Krstic, M., 2004, "Closed Form Boundary State Feedbacks for a Class of Partial Integro-Differential Equations," *IEEE Trans. Autom. Control*, **49**, pp. 2185–2202.
- [36] Jovanovic, M., and Bamieh, B., 2005, "Componentwise Energy Amplification in Channel Flows," *J. Fluid Mech.*, **534**, pp. 145–183.
- [37] Reddy, S. C., Schmid, P. J., and Henningson, D. S., 1993, "Pseudospectra of the Orr-Sommerfeld Operator," *SIAM J. Appl. Math.*, **53**(1), pp. 15–47.
- [38] Lee, D., and Choi, H., 2001, "Magnetohydrodynamic Turbulent Flow in a Channel at Low Magnetic Reynolds Number," *J. Fluid Mech.*, **439**, pp. 367–394.
- [39] Vazquez, R., Trelat, E., and Coron, J.-M., 2008, "Control for Fast and Stable Laminar-to-High-Reynolds-Numbers Transfer in a 2D Navier-Stokes Channel Flow," *Discrete Contin. Dyn. Syst., Ser. B*, **10**, pp. 925–956.
- [40] Sermange, M., and Temam, R., 1983, "Some Mathematical Questions Related to the MHD Equations," *Commun. Pure Appl. Math.*, **36**, pp. 635–664.
- [41] Cochran, J., and Krstic, M., 2008, "Motion Planning and Trajectory Tracking for the 3-D Poiseuille Flow," *J. Fluid Mech.*, in press.
- [42] Vazquez, R., and Krstic, M., 2008, "Control of 1-D Parabolic PDEs With Volterra Non-Linearities, Part I: Design," *Automatica*, **44**, pp. 2778–2790.
- [43] Vazquez, R., and Krstic, M., 2008, "Control of 1-D Parabolic PDEs With Volterra Non-Linearities, Part II: Analysis," *Automatica*, **44**, pp. 2791–2803.
- [44] Krstic, M., Magnis, L., and Vazquez, R., 2008, "Nonlinear Stabilization of Shock-Like Unstable Equilibria in the Viscous Burgers PDE," *IEEE Trans. Autom. Control*, **53**, pp. 1678–1683.
- [45] Krstic, M., Magnis, L., and Vazquez, R., 2009, "Nonlinear Control of the Viscous Burgers Equation: Trajectory Generation, Tracking, and Observer Design," *ASME J. Dyn. Syst., Meas., Control*, **131**(2), p. 021012.